Volume flow rate & velocity field

量測原理與機工實驗 (II)

熱流量測(3)

June, 01, 2011

Fu-Ling Yang

A. Volume flow rate

Volume/Mass flow rate (Averaged property)

- Field measurement: **Obstruction meters**

  Devices are implemented along the flow, which induces changes in flow pressure. The resulting pressure variation is then employed to extrapolate the flow velocity and the 'averaged' flow rate.

- Point measurement: intrusive type, **velocity probe**

  Transducer (pitot tube, piezo-sensor) are inserted into the flow which introduces a stagnation point to the flow of interest. The pressure variation at the stagnation point from the free stream indicates the stream velocity.

  Point velocity measurement at various locations

$$\dot{m} = \int_{\substack{\text{Duct}\\ \text{area}}} d\dot{m} = \int_{A} \rho U(x,y)\, dA = \sum_{i} \rho_i U_i A_i = \rho A U_{\text{avg}}$$

- Special methods for velocity or flow rate measurements:
  - thermal type (hot-wire), Turbine-type, pulse-producing methods

Obstruction meters

- The basic meter acts as an obstacle in the path of the flowing fluid, causing localized changes in the velocity. Concurrent pressure change occurs, which can be quantified in relation to the total (volume) flow rate

Bernoulli's equation $\frac{1}{2}U_1^2 + \frac{p_1}{\rho_1} + gz_1 = \frac{1}{2}U_2^2 + \frac{p_2}{\rho_2} + gz_2$

$A_1U_1 = A_2U_2 \quad (\rho_1 = \rho_2 = \rho)$ Incompressible flow

$$Q_{theoretical} = A_2U_2 = \frac{A_2}{\sqrt{1-(A_2/A_1)^2}}\sqrt{2\left(\frac{p_1}{\rho_1} + gz_1 - \frac{p_2}{\rho_2} - gz_2\right)}$$

$Q_{practucal} = C_V\, Q_{theoretical}$ **Velocity coefficient**

– Straightening vanes (honey cone) are often installed upstream to regulate the flow (reduce the lateral component of the mean flow, prevent large turbulent eddy to occur)

Obstruction meters, internal flow [1]

Venturi meter: entrance cone(21° span, flow acceleration) / short cylindrical throat / diffuser cone (5~15 ° span, flow deceleration)

–Small diffuser angle to minimize the loss from pipe friction, flow separation, and turbulence intensity (diminish total head loss)

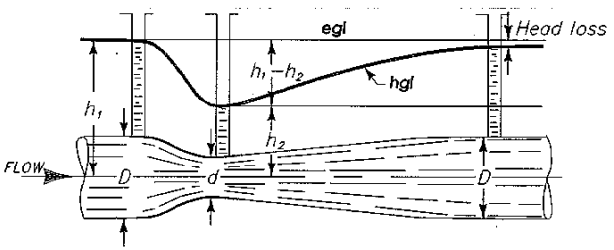

- Flow nozzle: a venturi meter without a diffuser cone

– Larger head loss, but lower cost with reliable error estimation of the throat pressure (~C_V)

Obstruction meters, internal flow [2]

- Orifice:

A plate with sharp-edged circular hole inserting in a flow. The pressure difference upstream / downstream of the orifice measures the total flow rate.

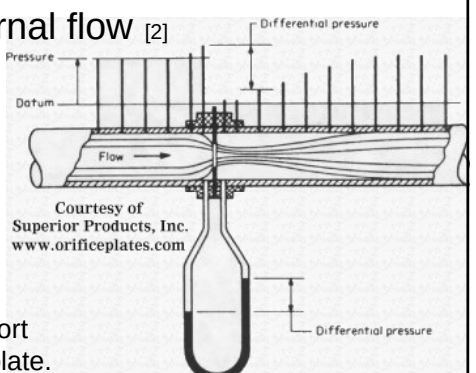

The streamlines tend to converge a short distance downstream from the orifice plate. A minimum flow area, **"contracted area of the jet"** or "**vena contracta**", is generated downstream of the orifice that acts as the throat in the nozzle or the venturi meter

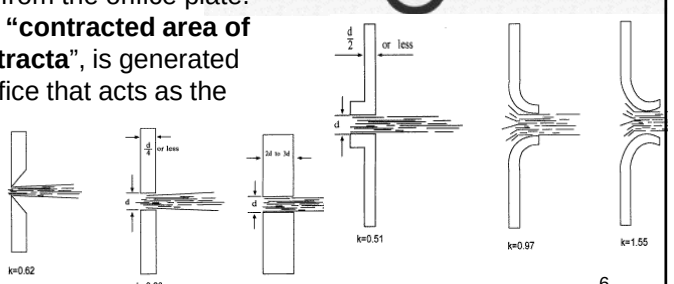

Obstruction meters, internal flow [2]

- Orifice:

Contraction coefficient C_C defines a throat area $A_2 = C_C A_0$ where A_0 is the orifice opening area

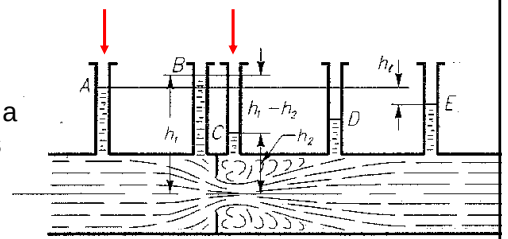

$$Q_{practucal} = \frac{C_V C_C A_0}{\sqrt{1-(C_C A_0/A_1)^2}} \sqrt{2\left(\frac{p_1}{\rho_1} + gz_1 - \frac{p_2}{\rho_2} - gz_2\right)} = CA_0\sqrt{2\left(\frac{p_1}{\rho_1} + gz_1 - \frac{p_2}{\rho_2} - gz_2\right)}$$

C: **orifice coefficient** depend on C_V, C_C, and orifice-to-duct area ratio A_0/A_1

-- The location of vena contracta changes with flow Reynolds number and area ratio (duct/orifice). Thus, pressure are usually measured 1D upstream (p1) and 1/2D downstream (p2) of the orifice.

Obstruction meters, internal flow [3]

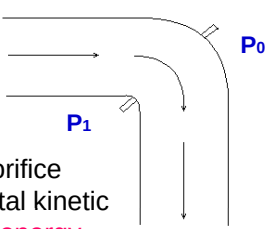

- Elbow meter
  - Contrasting to venturi meter, flow nozzle, and orifice meter that introduce head loss (deduction of total kinetic energy), elbow meter doesn't cause additional energy loss since it belongs to the flow itself.
  - Pressure rise resulted from centrifugal force is employed:

$$\frac{p_0}{\rho_0} + gz_0 = \frac{1}{2}C_k U_1^2 + \frac{p_1}{\rho_1} + gz_1$$

C_k: 1.3~3.2, depending on the size and the shape of the elbow

  - Volume flow rate: $$Q_{practucal} = A\overline{U} = \frac{A}{\sqrt{C_k}}\sqrt{2\left(\frac{p_0}{\rho_0} + gz_0 - \frac{p_1}{\rho_1} - gz_1\right)}$$

elbow meter coefficient $C = 1/\sqrt{C_k}$

  - Cons: needs to be calibrated on site

Obstruction meters, open channel flow [1]

- Important in navigation, flood control, irrigation
- Sluice Gate open-channel version of orifice meter
  - Flow through the gate exhibits jet contraction on the top surface, generating a vera contracta somewhere downstream of the gate.
  - Assume that no energy is lost and the pressure in vera contracta is hydrostatic, Bernoulli's equation can be applied for the streamline on the free surface, with respect to the flow ground

$$\frac{1}{2}U_1^2 + \frac{p_1}{\rho_1} + gy_1 = \frac{1}{2}U_2^2 + \frac{p_2}{\rho_2} + gy_2$$

$$+A_1U_1 = A_2U_2$$

$$\Rightarrow Q_{practucal} = C_V A_2 U_2 = \frac{C_V C_C A}{\sqrt{1-(y_2/y_1)^2}}\sqrt{2g(y_1-y_2)}$$

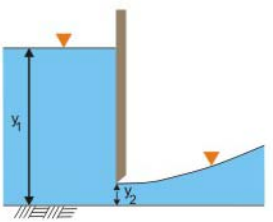

--Depending on C_V,C_C, y_2/y_1, and (y_2-y_1)
-- Linear proportion to A, gate opening area

Obstruction meters, open channel flow [2]

- Weir, an obstruction in an open channel over which fluid flows
  - Total flow rate depends on the **weir head** (vertical elevation of the weir crest from undisturbed region) and the geometry

$$\frac{1}{2}U_1^2 + \frac{p_1}{\rho_1} + gH = \frac{1}{2}U_2^2 + \frac{p_2}{\rho_2} + g(H-h)$$

$$U_2 = \sqrt{2gh+U_1^2} \approx \sqrt{2gh}$$

$$\Rightarrow Q_{theoretical} = \int_A U_2 dA = \int_0^H \sqrt{2gh}\, W dh = \tfrac{2}{3}\sqrt{2g}\, W h^{3/2}$$

$$\Rightarrow Q_{practical} = C_D Q_{theoretical}$$

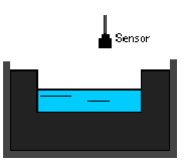

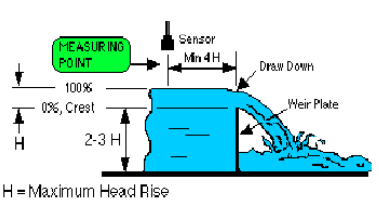

Weir discharge coefficient C_D:

drawdown contraction from the top free surface, friction loss in the flow, velocity components being other than horizontal

Obstruction meters, open channel flow [2]

- Triangular Weir (V-notch weir),
  –often employed for small flow rates.
  –Higher accuracy is achieved: the averaged width of the flow section increases as the head increases.

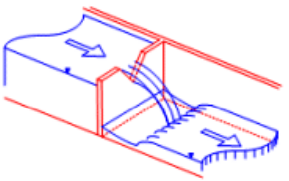

$$\Rightarrow Q_{practical} = \frac{8}{15}\sqrt{2g}\,\tan\left(\theta/2\right)C_D H^{5/2}$$

** Note that: Physical corrosion and surface causes rough weir surface and rounded frontal edge, which may further increase the C_D due to reduction in flow contraction.

Transverse weir:

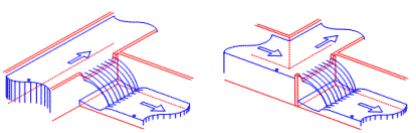

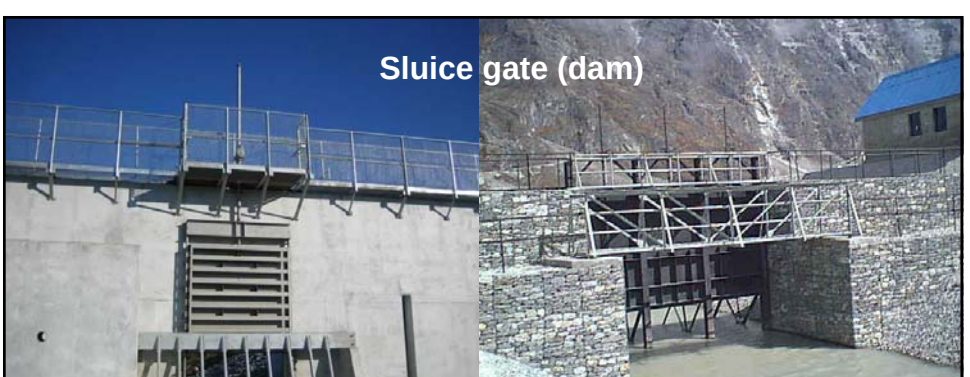

Weir

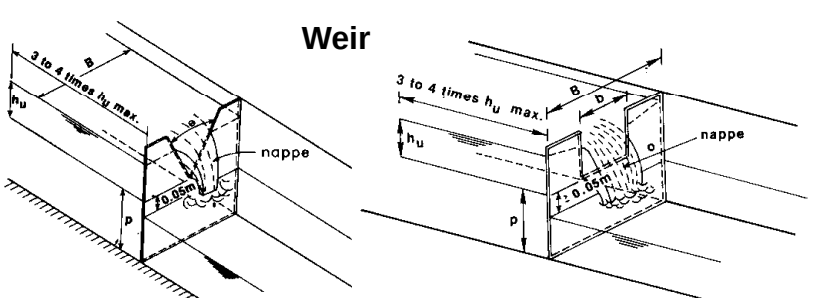

B1. Velocity (point measurement)

Variable-area meter

--drag-force velocity transducer

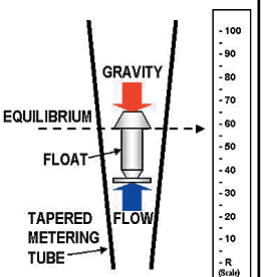

- Principle employed: the drag force on a body in a uniform and steady flow is well investigated $F_D = C_D \frac{1}{2}\rho U^2 A$

- **Rotameter:** upright tapered tube + float bob

$$C_D \tfrac{1}{2}\rho_f U^2 A_b + \rho_f V_b g = \rho_b V_b g \Rightarrow U = \cdots$$

mean velocity of the flow in the annual space between the float and the tube

- Mass flow rate: $A_{annulus} = \frac{\pi}{4}\left[(D+ay)^2 - d^2\right] \approx \frac{\pi}{2} Day$

$$\dot{m} = \rho_f A_{annulus} U = \frac{\pi}{2} Day \sqrt{\frac{2V_b g}{C_D A_b}\left(\rho_f - \rho_b\right)\rho_f} = K\sqrt{\left(\rho_f - \rho_b\right)\rho_f}\, y$$

Sensitivity to fluid density can be minimized by using $\rho_b \geq 2\rho_f$

Pipe flow (Poiseuille flow)

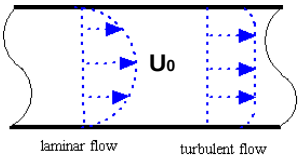

Laminar flow $U(r) = U_0\left[1-\left(\frac{r}{R}\right)^2\right]$

$$\dot{m} = \rho U_0 \int_0^{2\pi}\int_0^R \left(1-\left(\frac{r}{R}\right)^2\right) r\,dr\,d\theta = \rho\pi R^2 \frac{U_0}{2} = \rho A U_{\text{avg}} \quad \Rightarrow U_{\text{avg}} = \frac{U_0}{2}$$

Fully-developed **turbulent flow** in a smooth pipe $U(r) = U_0\left(1-\frac{r}{R}\right)^{1/n}$ $\qquad n = \text{fct}(\text{Re}_{\text{avg}}),\ \text{Re}_{\text{avg}} = \frac{\rho D U_{\text{avg}}}{\mu}$

$$U_{\text{avg}} = \frac{2\pi^2}{(n+1)(2n+1)} U_0 \qquad \dot{m} = \rho A U_{\text{avg}}$$

Note that accurate flow rate measurement can be inferred from velocity measurement at a point only if the flow profile is completely known.

Turbine meter

- A wheel with cup-type / propeller-type blades rotate when exposed to a free stream. The number of turns of the wheel is linearly proportional to the free stream velocity.
- Conventionally, permanent magnet is inserted to the blades and each time it passes the pole of the coil installed on the outer casting, a voltage pulse is generated.
- Pros: easy to use/ implement, cheap
- Cons: frequent bearing maintenance, loss of accuracy at low flow rates

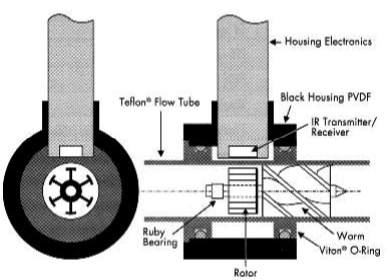

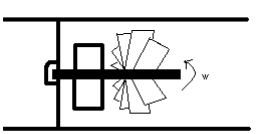

Pulse-generating method --vortex-shedding transdu

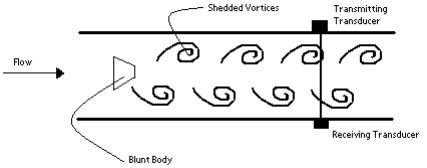

- When a symmetrical bluff body is placed in the stream, with its axis aligned with the tube axis, vortices are formed and shed alternatively on both sides of the body.
- The shedding frequency or the frequency of formation, ***f***, is a function of flow rate and can be related to body diameter, ***D***, flow velocity, U_0, through a dimensionless number:

Strouhal number $$Str = \frac{f\,D}{U_0}$$

Strouhal number remains nearly constant (~0.2) over a wide range of body Reynolds number (300 to 150,000)→ $U_0 = f\,D / Str$

To sense the shedding vortices , ***f*** : measure vibration of the body, monitor the deformation of diaphragm installed downstream on both sides of the body, monitor the temperature variation of thermistors inserted to the flow

Direct / Intrusive measurement

1: Pitot tube
2: Hot-wire anemometer

- Pitot tube
  - Measure the velocity magnitude

$$\frac{1}{2}U^2 + \frac{P}{\rho} + gz = const$$

$$\frac{1}{2}U_1^2 + \frac{P_1}{\rho} + gz_1 = \frac{1}{2}U_2^2 + \frac{P_2}{\rho} + gz_2$$

$$\frac{1}{2}U_0^2 + \frac{P_{Static}}{\rho} + gz_1 = \frac{P_{Stag.}}{\rho} + gz_2$$

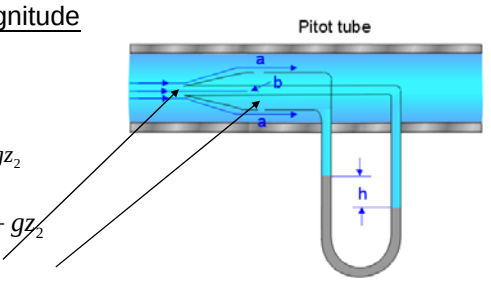

$$U_0 = \sqrt{\frac{2\left(P_{Stag.} - P_{Static}\right)}{\rho} + 2g\left(z_2 - z_1\right)} \approx \sqrt{\frac{2\left(P_{Stag.} - P_{Static}\right)}{\rho}}$$

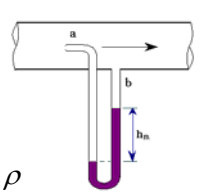

Stagnation / Static pressure

  - Error: from the measurements of P_{stag}, P_{static}, and ρ

Flow direction detector

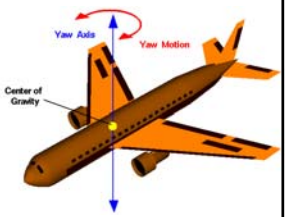

- Principle:
  - non-uniform pressure distribution across the tube surface.

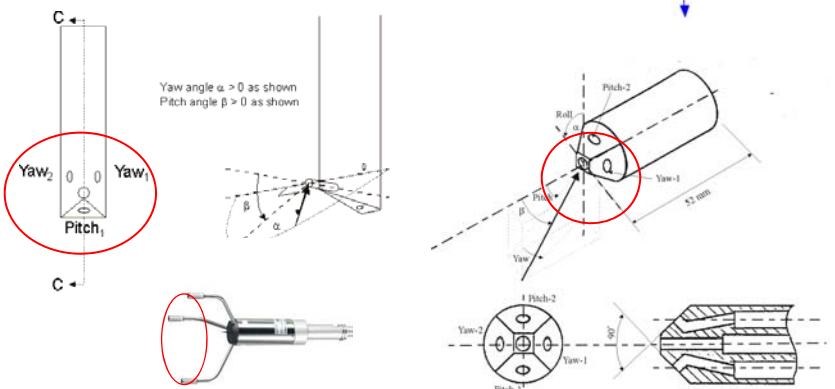

Claw style: point measurement possible

Manometer dynamics

- Upon any pressure change in one end

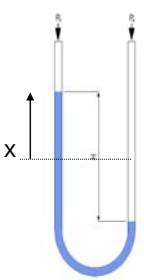

$$m_L \ddot{x} = \pi R^2 (p_A - p_B) - \pi R^2 (2x\rho g) - 2\pi RLf$$

Effective column mass $m_L = \rho \frac{4}{3} \pi R^2 L$

Wall shear stress $f = \frac{4\mu \dot{x}}{R} = \frac{4\mu \bar{U}}{R} \sim \mu \frac{du}{dy}$

$$\frac{2L}{3g}\ddot{x} + \frac{4\mu L}{R^2 \rho}\dot{x} + x = \frac{p_A - p_B}{2\rho}$$

Mass-spring-damper system (2nd order ODE)

Averaged flow velocity; from Hagen-Poiseuille circular pipe flow:

$$0 = -\frac{\partial p}{\partial x} + \mu \frac{\partial}{\partial r}\left(r \frac{\partial U}{\partial r} \right) \qquad Q = \int_{r=0}^{R} 2\pi r U(r) dr = -\frac{\pi R^2}{8\mu}\left(\frac{\partial p}{\partial x} \right) = \bar{U} \pi R^2$$

$$U = -\frac{1}{4\mu}\left(\frac{\partial p}{\partial x} \right)\left(R^2 - r^2 \right) \qquad \bar{U} = -\frac{1}{8\mu}\left(\frac{\partial p}{\partial x} \right) \sim -\frac{1}{8\mu}\left(\frac{p_A - p_B}{L} \right)$$

Hot-wire,-film anemometers (熱線測速計)

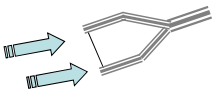

- Principle: energy conservation law:

heat generation = heat convection to free stream

$$P = I^2 R_w = hA_w(T_w - T_f)$$

Thermal-electric property

$$R_w(T_w) = R_0\left[1+\alpha(T_w - T_0)\right]$$

Heat transfer coefficient

King's law: $h = a + bU_f^c$

$(c \sim 0.5)$

$$a + bU_f^c = \frac{I^2 R_0\left[1+\alpha(T_w - T_0)\right]}{A_w(T_w - T_f)}$$

Two types: Constant current I ; Constant temperature T_w

Hot-wire,-film anemometers

- Constant Current type
  - Large current: high sensitivity
  - Burn-out concern: heat accumulation with sudden flow slowdown
- **Constant Temperature type**
  - Rely on rapid Feedback control
  - More popular for its reduced sensitivity to flow variations

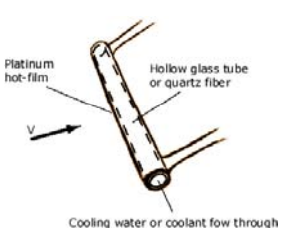

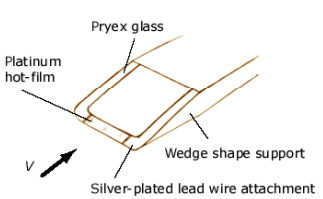

- **Measure the velocity <u>perpendicular to the wire.</u>**

Hot-wire/film anemometer

- **Pros:**
  - Excellent spatial resolution (small in size)
  - High frequency response (thermal-electric property)
- **Cons:**
  - Fragile, low mechanical strength
  - Expensive
  - Surface contaminant (dust, chemical) that changes the thermal/ electrical characteristics R_w, h of the system. Thus, frequent calibration is required.
  - Vibration (especially when used in high speed flow)
  - In general, not applicable in electrically conducting fluids!

LDA, LDV—Laser Doppler Anemometer, Velocimetry

- Dual-beam system
  'Focal point' is generated by focusing two laser beams, of equal intensity and wave length, at the point of interest.

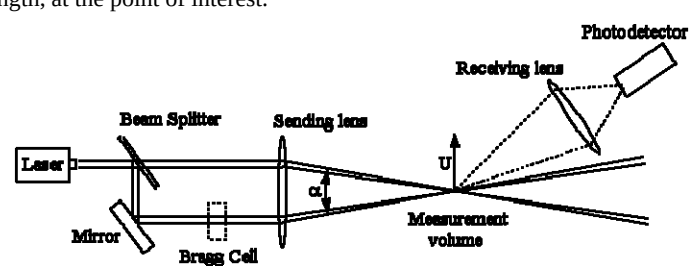

Interference fringe pattern is generated at the focal point.

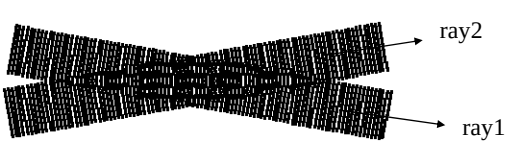

LDA, LDV—Laser Doppler Anemometer, Velocimetry

- Doppler effects when there is relative velocity between the wave source and the observer:

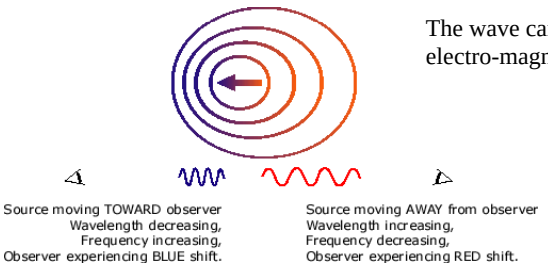

The wave can be either acoustic or electro-magnetic radiation wave.

- Doppler formula:

-- monochromatic light source (of single frequency ***f***, wavelength λ, speed of light $c = \lambda f$)

-- A observer is at a distance ***L*** from the stationary source , it takes the wave ***n*** cycles to propagate to the observer, where $n = L / \lambda$

Doppler formula for a moving source

- If the source is moving towards the observer at velocity ***V***, the distance that the wave train needs the travel to arrive at the observer is shortened, from ***L*** to

$$L - V(\Delta t) = L - V\left(\frac{L}{c}\right) = (1 - V/c)L$$

- Same number of waves, n, are emitted no matter the source is moving or not. Thus the modified wave length can be calculated according to the motion of the source:

$$n = \frac{L}{\lambda} = \frac{(1 - V/c)L}{\lambda_{Blue}} \quad \Rightarrow \quad \begin{cases} \lambda_{Blue} = (1 - V/c)\lambda \\ \lambda_{Red} = (1 + V/c)\lambda \end{cases}$$

- Since the light speed is constant (if travels in the same medium), the observed frequency is shifted as the inverse of the modified wave lengths:

$$c = f\lambda = f_{Blue}\lambda_{Blue} = f_{Red}\lambda_{Red} \quad \Rightarrow \quad \boxed{f_{\substack{Blue \\ Red}} = \frac{f}{(1 \pm V/c)}}$$

LDA, LDV—Laser Doppler Anemometer, Velocimetry

- When the particle moves through the fringe, it reflects light (burst signal) to the photodetector. The received information will be analyzed to estimate the tracer particle (and hence the flow) velocity.

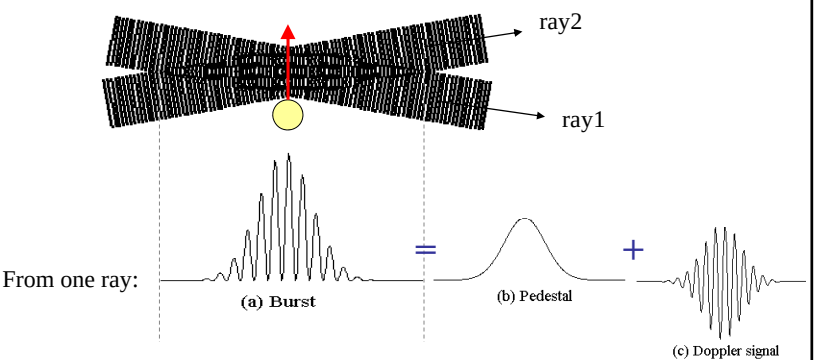

(b) Positive offset due to two forward scattering beam. (Low frequency signal that contains no info of the particle motion). Subtracted to obtain the desired Doppler signal.

LDA, LDV—Laser Doppler Anemometer, Velocimetry

-- Recall Doppler shift of the scattered light from a moving object.

Since the particle intercepts the two laser beams at different angles, the resulting Doppler shift is different from the two rays.

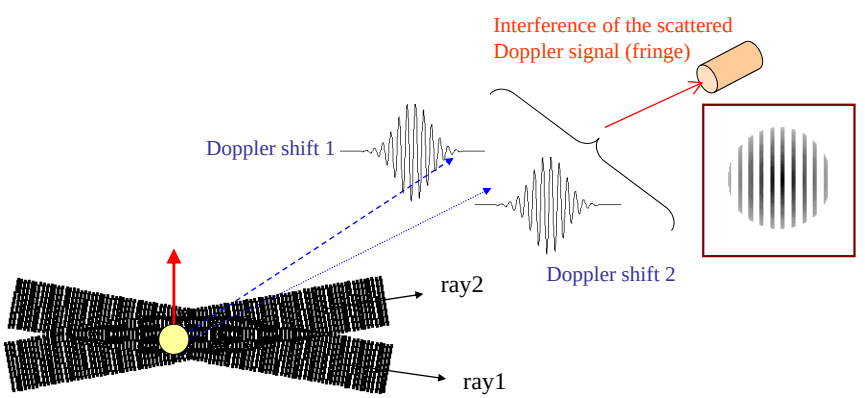

LDA, LDV—Laser Doppler Anemometer, Velocimetry

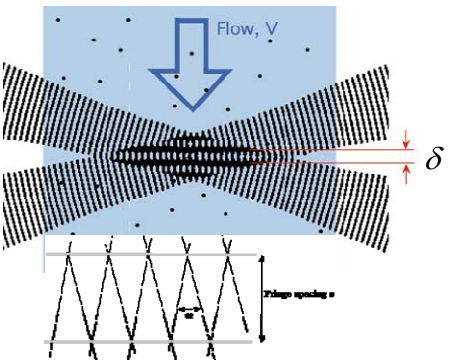

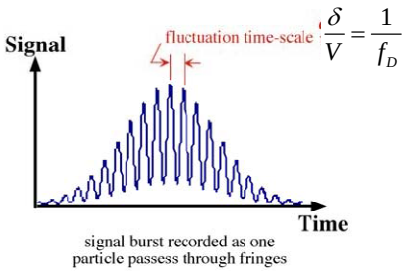

$$\frac{\delta}{V} = \frac{1}{f_D}$$

f_D **measured signal frequency (Doppler shifted)**

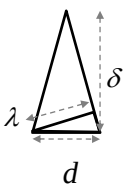

$$\frac{\delta}{d/2} = \frac{\lambda}{d\sin(\theta/2)}$$

$$\Rightarrow \quad \delta = \frac{\lambda}{2\sin(\theta/2)}$$

$$V = f_D\delta = \frac{f_D\lambda}{2\sin(\theta/2)}$$

LDA LDVs

- Errors sources:
  - Particle averaging bias
    - More particle passages for faster flows
    - Higher variance (recall the positive burst signal) gives a higher mean.
    - Still an open question on how to offset the bias…
  - Velocity gradient broadening
    - With background velocity gradient, successive particles will have difference velocity when entering focal point
    - Thus, even for a steady flow (under steady shearing for example), the measured signal tends to have higher variance than that obtained from a uniform flow.
  - Finite transit time broadening
    - Resulting from too few fringes in the measured volume at the focal point.
    - Need to match both the tracer particle size and laser wavelength, as well as the characteristic particle velocity and laser frequency (signal frequency).

B2. Velocity (field distribution)

Schlieren image system

- **Schlieren** are optical in-homogeneities in transparent material not visible to the human eyes.
- These localized in-homogeneities result in differences in the refractive index of the medium. Thus, a uniform light ray passing through this in-homogeneous medium will be deviated. (**Chromatic Aberration**)

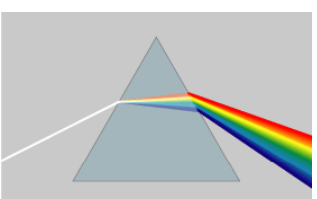

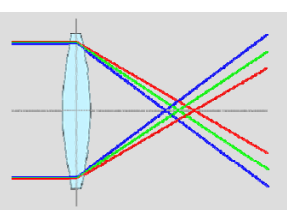

- A schlieren system (lense system) is developed to covert the deflected light into shadow visible to human eyes.

Chromatic aberration (色差)

- Refraction of light– different transmission velocity in different medium

$$n = \frac{c}{\mathrm{v}}$$ Light speed in vacuum

Speed of light in a specific medium $\mathrm{v} = f_{\text{medium}}\lambda_{\text{incident}}$

$$n = \frac{c}{f_{\text{med.}}\lambda_{\text{i}}} \propto \frac{1}{\lambda}$$

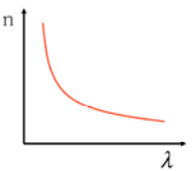

- Snell's law

$$n_1 \sin\theta_1 = n_2 \sin\theta_2$$

$$\sin\theta_i \sim \frac{1}{n_i} \sim \lambda_i$$

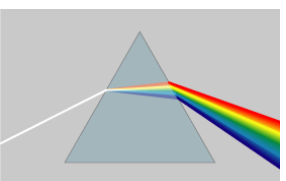

Principles of schlieren photography

- Schlieren photography refers to the 'image conversion' for the schlieren of a fluid medium of **varying density**.
- **Gladstone-Dale empirical relation**: $n-1 = K\rho_{\text{medium}}$ (K is a very weak function of wavelength)
- For an ideal gas, $n-1 \propto \frac{p}{RT}$

$$\Rightarrow \boxed{\sin\theta \propto T}$$

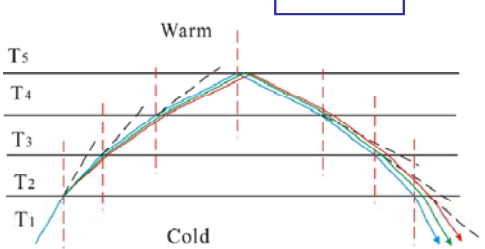

Shadowgraph

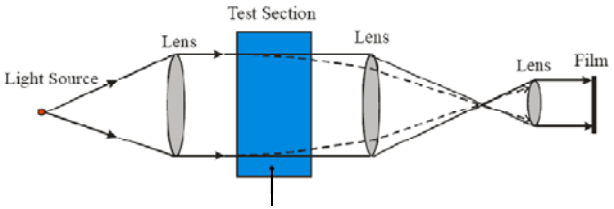

- **Deviation in *n* due to local density variation.**
- Gladstone-Dale equation: $n-1=K\rho_{\text{medium}}$
- Shadow patterns form when both the deflected (distorted) and the light rays are projected onto the viewing screen.
- The bright and the dark regions represent the expansion and the compression flow regimes in the test section.

Schlieren Photograph

- Similar to shadowgraph, only the deflected light rays for further manipulated at the focal point, using
  - Schlieren Knife edge (opaque)
  - filter array (transparent)

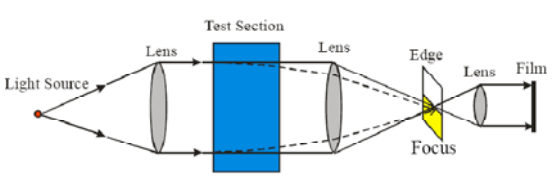

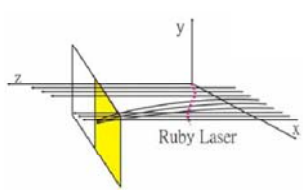

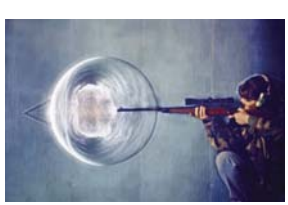

Light refraction mechanism

- Temperature difference
- Concentration difference
- non-uniform medium composition
- Shock wave (compressibility of the medium)…

Schlieren imaging system:

- Pros: low cost with high sensitivity
- Cons:
  - limited observation field (by the size of the lenses and the optical system);
  - difficult system set-up;
  - requires sufficient density change (refractive changes)

Schlieren examples

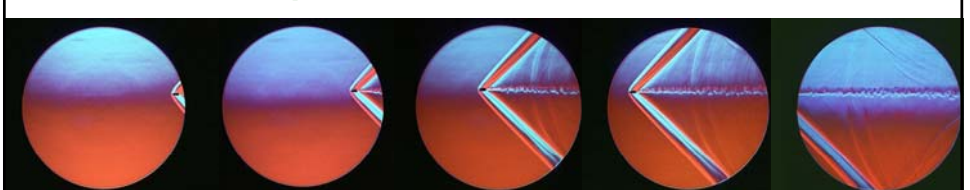

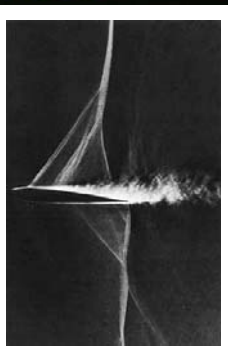

Transonic flow over an airfoil. The nearly vertical shock wave is followed by boundary layer separation that adversely affects lift, drag, and other flight parameters.

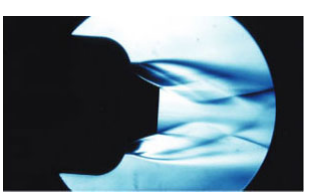

Exhaust from a new type of nozzle for reusable rockets

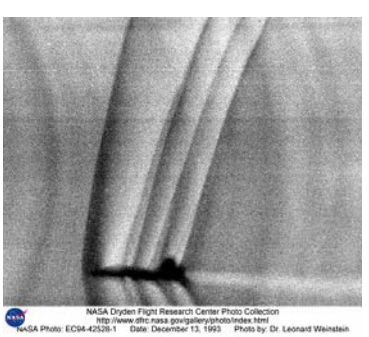

Schlieren photograph of T-38 shock waves at Mach 1.1, 13,000 feet

PIV—Particle Image Velocimetry

- Basics:
  - The fluid is seeded with florescent dye (that becomes visible when excited by a light source of a specific frequency)
  - Laser + optics to generate a 'laser sheet' that cuts through the flow (observation plane)

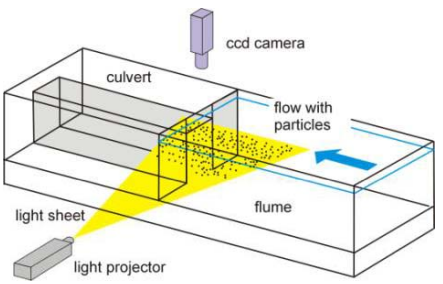

  - Image acquisition system
  - Image processing is followed for quantitative analysis.

PIV—Particle Image Velocimetry

- The pulsed laser of nano-second duration shed consecutive light rays on the flow at ~15HZ frequency (rate/duration depends on the type of laser).
- The illuminated flow field at both time t and $t+dt$ is stored into a Double-framed digital image for subsequent image analysis.

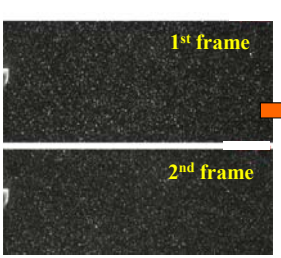

- Cross-correlation of the avg. displacement of the seeding particles determine the flow velocity vector.

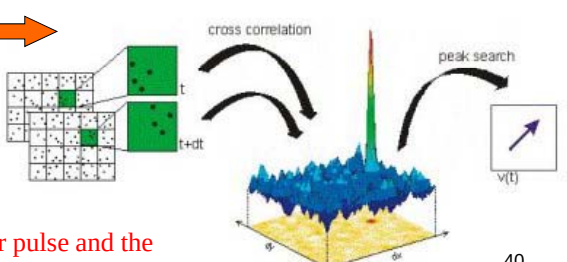

** Synchrony between the laser pulse and the image acquisition is crucial for flow analysis.

PIV correlation scheme

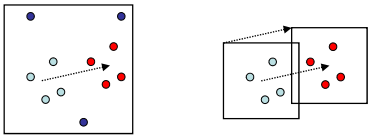

- Many correlation schemes exist.
- For standard cross-correlation, the motion of the majority of particles in an **interrogation window** must be contained within the interrogation window. At the same time, the particle motion must be large enough to resolve small deviations (eg: Brownian motion of the seeding particles). Thus, large interrogation window is often required which implies large computation.

- **Window shifting** and **Multi-pass** techniques help improve the situation:
  - With *a priori* knowledge of the flow, the second interrogation window may be shifted a discrete amount, equivalent to the mean motion, a higher percentage of particles will be captured, resulting in greater correlation peaks and lower noise.
  - Alternatively, a second (shifted) correlation can be performed using the result of the first (unshifted) correlation. This is a multi-pass technique. The second and/or subsequent passes can also therefore use smaller windows since the motion will be contained by the window shift.

PIV for bio-fluid research

Images are from Dr. E. Drucker at UC Irvine
http://darwin.bio.uci.edu/~edrucker/home/index.htm

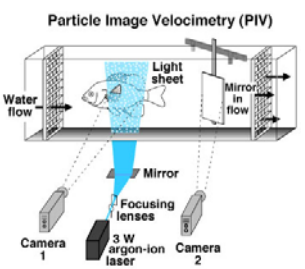

- Image analysis on the tracer particle:
  - A vector field of flow velocity is generated.

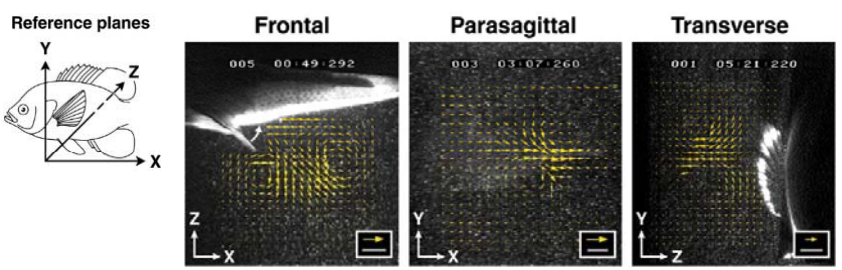

  - Reliable results require images of high quality!

Major challenge of today's PIV

- PIV critically relies on the averaging particle motion within an interrogation window. Thus, if severe velocity gradients exist within the window, error arises.

- New algorithm has been developed using deformed interrogation window with the associated distorted correlation peaks. This is quite effective, but computationally expensive. (Of the order five times the correlation time of default multi-pass schemes.)